Bioorganic & Medicinal Chemistry 20 (2012) 1298–1302

Contents lists available at SciVerse ScienceDirect

Bioorganic & Medicinal Chemistry

journal homepage: www.elsevier.com/locate/bmc

Characterization of a 1,4-disubstituted 1,2,3-triazole binding to T box antiterminator RNA

S. Zhou [a], J.A. Means [b], G. Acquaah-Harrison [a], S.C. Bergmeier [a], J.V. Hines [a,*]

[a] Department of Chemistry and Biochemistry, Ohio University, Athens, OH 45701, USA
[b] University of Rio Grande, Rio Grande, OH 45674, USA

ARTICLE INFO

Article history:
Received 13 October 2011
Revised 5 December 2011
Accepted 10 December 2011
Available online 16 December 2011

Keywords:
Triazole
RNA
Ligand binding
T box riboswitch
Antitermination

ABSTRACT

The T box riboswitch regulates the transcription of many bacterial genes by structurally responding to cognate non-aminoacylated (uncharged) tRNA. The riboswitch contains multiple conserved RNA elements including a key structural element, the antiterminator, which binds the tRNA acceptor end nucleotides. Previous studies identified a lead 1,4-disubstituted 1,2,3-triazole, GHB-7, that disrupted formation of a tRNA–antiterminator RNA model complex. The affinity and molecular interactions of GHB-7 binding to antiterminator model RNA were characterized as part of a comprehensive T box antiterminator RNA-targeted drug discovery project. In-line probing, UV-monitored thermal denaturation and docking studies all consistently indicated that GHB-7 likely binds to the bulge region of the antiterminator, reduces the flexibility of the bulge nucleotides and, overall, stabilizes the RNA secondary structure. These results begin to elucidate possible mechanisms for ligand-induced inhibition of tRNA binding to T box antiterminator RNA and contribute to the knowledge of how small molecules bind relatively simple RNA structural elements such as bulges.

1. Introduction

Riboswitches are noncoding RNAs that regulate gene expression by responding to a metabolic effector molecule in a structurally unique manner and affecting the transcription or translation of the mRNA encoded by the gene.[1,2] The T box transcription antitermination riboswitch regulates the transcription of vital genes in many Gram-positive bacteria,[3,4] thus making it a medicinally relevant target for drug discovery. As part of a comprehensive drug discovery initiative, we have been investigating ligand features that are critical for binding a highly conserved element within the T box riboswitch called the antiterminator.[5–12]

The T box riboswitch is located in the 5′-untranslated region (5′-UTR) of the mRNA of T box regulated genes and involves multiple conserved RNA elements that specifically bind and structurally respond to cognate non-aminoacylated (uncharged) tRNA.[4] The tRNA anticodon forms base pairs with a specifier sequence in Stem I of the 5′-UTR while the tRNA acceptor end nucleotides base pair with nucleotides in the bulge of a unique structural element called the antiterminator (Fig. 1a).[4] This tRNA–antiterminator base pairing is essential for transcription antitermination to occur and results in transcription of the full mRNA (including the protein encoding region).[13] In the absence of uncharged cognate tRNA, an alternative terminator structural element forms and transcription terminates before the protein coding region is transcribed, thus leading to a truncated, incomplete, mRNA.[14]

Based on a phylogenetic analysis of T box riboswitches there is a high level of sequence and structural conservation in the antiterminator.[15,16] This phylogenetic conservation, along with the critical role the antiterminator plays in the medicinally relevant T box riboswitch, make the antiterminator an important RNA target for drug discovery. We previously reported the screening of a series of triazole ligands for binding to the antiterminator[9] and have identified several that significantly disrupt the tRNA–antiterminator complex.[12] In this paper we characterize the binding interaction between the antiterminator and a lead 1,4-disubstituted 1,2,3-triazole, GHB-7 (Fig. 1b). These studies are critical for further potential

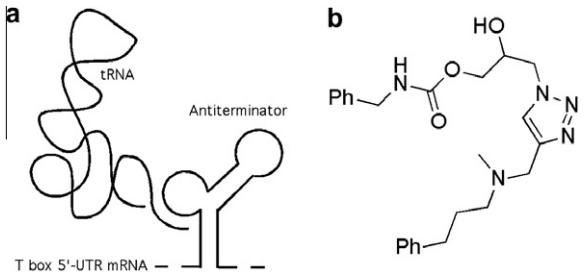

Figure 1. (a) Schematic of tRNA acceptor end binding to the antiterminator element in the T box riboswitch 5′-UTR. The tRNA anticodon also binds to the Stem I region of the 5′-UTR (not shown).[4] (b) 1,4-Disubstituted 1,2,3-triazole, GHB-7.

* Corresponding author. Tel.: +1 740 593 9464.
E-mail address: hinesj@ohio.edu (J.V. Hines).

0968-0896/$ - see front matter © 2011 Published by Elsevier Ltd.
doi:10.1016/j.bmc.2011.12.017

development of T box antiterminator-targeted medicinal agents and for contributing to the knowledge base of known RNA–ligand interactions in general.

2. Results and discussion

We previously reported a fluorescence-based, single concentration binding assay of a series of 1,4-disubstituted 1,2,3-triazoles binding to T box riboswitch antiterminator model RNA, AM1A.[9] Fluorescence anisotropy screening assays identified lead compounds that also disrupted tRNA from binding.[12] One of these lead compounds, GHB-7, significantly disrupted tRNA binding to AM1A resulting in a 79% decrease in anisotropy of the tRNA–AM1A complex at [GHB-7] = 100 μM.[12] The studies reported here investigate, at a molecular level, the binding of GHB-7 to AM1A in order to determine the ligand features that likely contribute to inhibition of tRNA binding to the T box antiterminator model RNA.

2.1. Ligand affinity for antiterminator RNA

Preliminary screening studies indicated that GHB-7 likely bound antiterminator model RNA, but no binding constant was determined due to the nature of the single concentration screening assay.[9] Consequently, the affinity of GHB-7 binding to T box antiterminator model RNAs (Fig. 2a) AM1A and C11U (a reduced function variant)[17] was determined using a previously developed fluorescence resonance energy transfer (FRET) binding assay.[5,7] GHB-7 bound AM1A and C11U with similar affinity based on the observed K_d values of 56 ± 16 and 59 ± 10 μM, respectively (Fig. 2b). This is in contrast to binding studies for a series of 4,5-disubstituted oxazolidinones in which ligands bound AM1A and C11U with differing affinities.[7]

Given that the GHB-7 affinity for AM1A and C11U is comparable, it is likely that GHB-7 binding does not involve direct contact with the nucleotide base at position 11. In addition, the affinity of GHB-7 for AM1A is weaker than that of the oxazolidine ligands that bind AM1A,[7] but is comparable to the affinity of the aminoglycoside paromomycin binding to AM1A.[5] Aminoglycosides are known to bind AM1A predominantly via electrostatic interactions,[5,8,18–20] yet GHB-7 has only one nitrogen that could be protonated at physiological pH compared to five for paromomycin. This would appear to indicate that the GHB-7 affinity is due to additional binding interactions other than just electrostatic attraction.

2.2. Ligand effect on antiterminator RNA stability

A UV-monitored thermal denaturation study[21] of AM1A both with and without GHB-7 was conducted to characterize the extent to which GHB-7 affected the stability of AM1A (Fig. 2c). The melting temperature (T_m) of AM1A increased from 51 to 52 °C in the presence of GHB-7 (100 μM). In addition, a distinct additional peak was observed in the presence of GHB-7 with an apparent T_m = 69 °C.

The T_m data indicate that some stabilization of AM1A occurs in the presence of GHB-7 as evidenced by the increased T_m of the main peak and the appearance of an additional peak with a higher T_m. This apparent ligand-induced stabilization is consistent with a recently reported high-throughput screening assay in which GHB-7 was identified from a library of triazole compounds as significantly increasing the T_m of fluorescently labeled AM1A.[22] The increased T_m in both the UV-monitored thermal denaturation studies reported here and the previously reported high-throughput thermal denaturation studies[22] indicate that GHB-7 likely binds in a manner that stabilizes the overall secondary structure of AM1A.

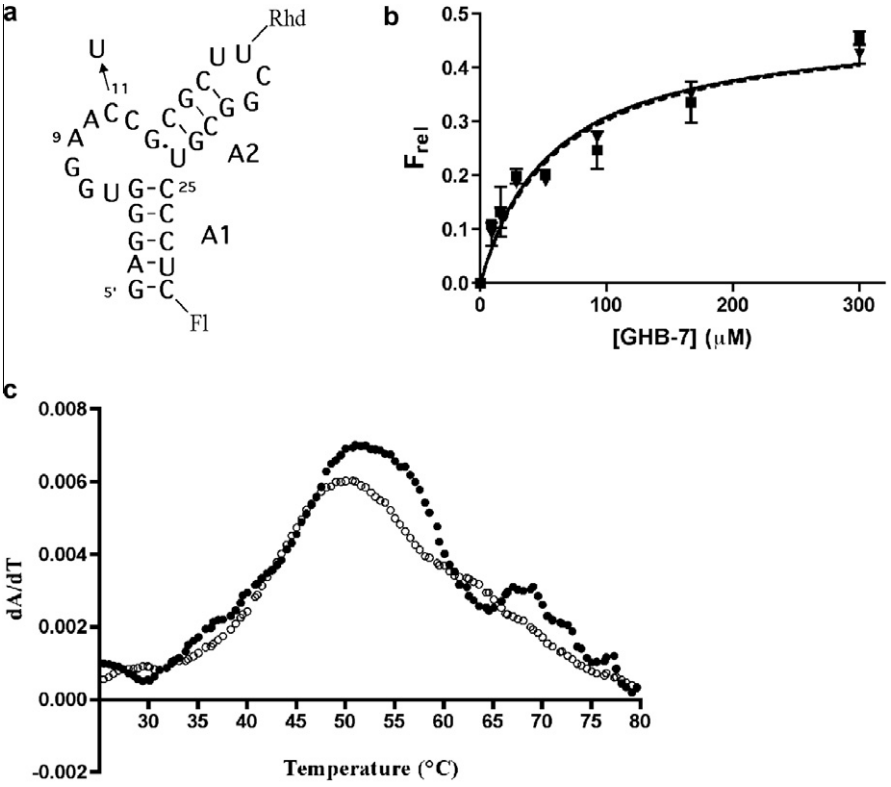

Figure. 2. (a) FRET-labeled antiterminator model RNA AM1A and C11U (C to U variation at position 11 noted by arrow), (b) binding isotherm of GHB-7 binding to FRET-labeled AM1A (square symbol, solid line) and C11U (triangle symbol, dashed line). $F_{rel} = |F-F_o|/F_o$, $R^2 = 0.9$ (c) UV-monitored thermal denaturation of AM1A without (open circle) and with (filled circle) GHB-7 (100 μM).

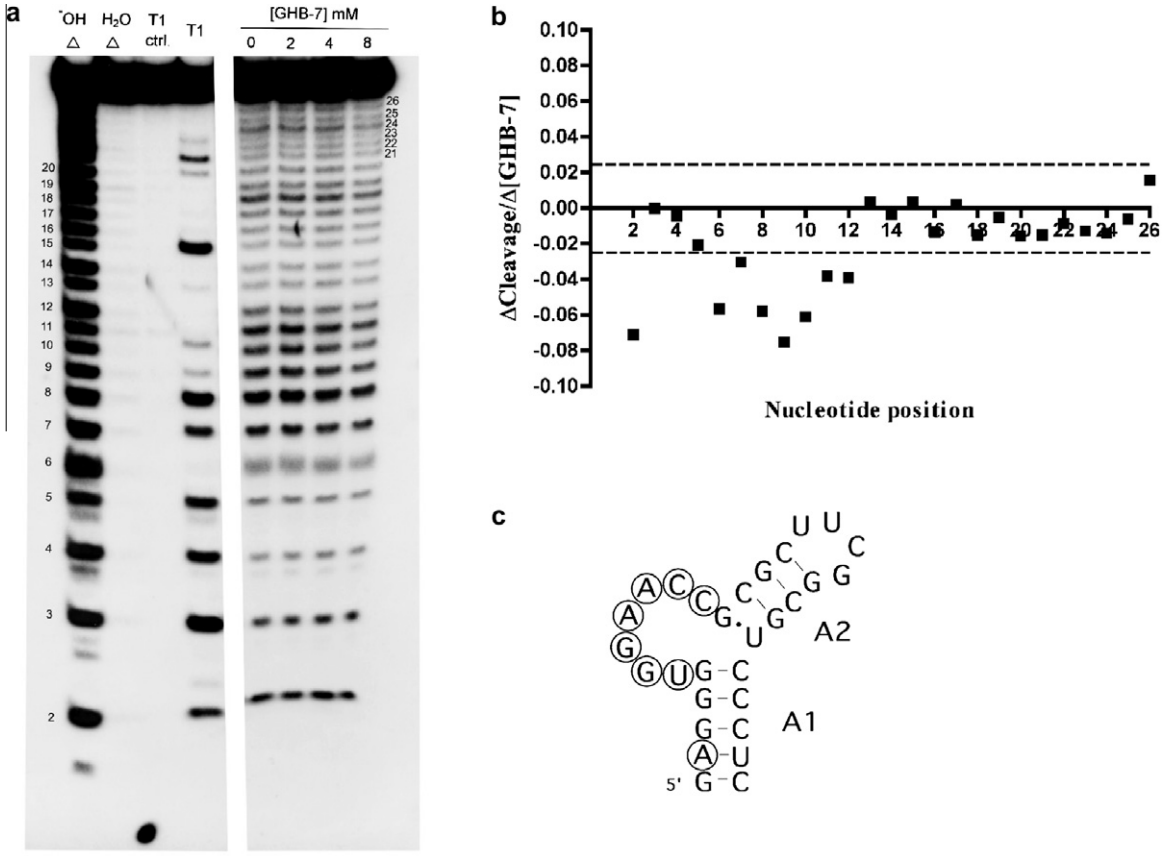

Figure. 3. In-line probing of GHB-7 binding to AM1A. (a) autoradiograph, (b) plot of slope of concentration-dependent cleavage patterns where dashed lines represent average of absolute value of slope for all nucleotide positions. (c) Secondary structure of AM1A with most significant ligand-induced decreases in in-line cleavage indicated by open circles.

2.3. Ligand-induced changes in RNA nucleotide flexibility

In-line probing experiments[23] of AM1A in the presence of GHB-7 were performed to determine if a change in the secondary structure occurred upon ligand binding. No increase in cleavage was observed at any of the positions (Fig. 3) indicating that there was no significant increase in single-stranded nature or flexibility of the RNA in the presence of the ligand. Instead, a decrease was observed at several nucleotides, most notably U6-C12, the nucleotides in the bulge region. A decrease in in-line cleavage is indicative of the ligand binding and decreasing the nucleotide flexibility.[23]

Based on the in-line probing results, the overall secondary structure of the RNA did not change dramatically in the presence of the ligand. Instead, the decreased in-line cleavage observed from U6-C12 indicates that the ligand possibly reaches across the bulge in AM1A, thus reducing the overall conformational flexibility of the entire bulge region. This is consistent with the ligand-induced stabilization observed in the thermal denaturation studies (Section 2.2).

2.4. Ligand-antiterminator RNA docking

Docking studies were carried out to determine the possible GHB-7 binding interactions that might occur with AM1A. Glide (Macromodel) was used to perform flexible ligand docking of the mono-protonated GHB-7 to the NMR-derived solution structure of AM1A[24] (PDB ID = 1N53). Previous studies have indicated that this docking method provides useful insight into possible contacts when ligand binding does not substantially rearrange the overall structure of the RNA.[11] Since the in-line probing results indicate that there is no large change in secondary structure upon GHB-7 binding (Section 2.3), this method was used to dock GHB-7 enantiomers to the solution structure of AM1A and determine possible binding interactions.

The energetically most stable docked ligand–RNA complex was with the *S* enantiomer of the mono-protonated GHB-7 (E_{model} = −126.6 kcal/mol). The complex of the *R* enantiomer with AM1A had reduced predicted stability (E_{model} = −122.9 kcal/mol). Both enantiomers docked in the bulge region of AM1A with contacts reaching from the 5′ to the 3′ end of the bulge (Fig. 4) consistent with the in-line cleavage results (Section 2.3). Both enantiomers formed a hydrogen bond between the hydroxyl group of GHB-7 and a 5′ phosphate oxygen of U24, as well as, a hydrogen bond between the protonated amine of GHB-7 and a 5′ phosphate oxygen of G8. The most stable ligand complex (with the *S* enantiomer) involved π–π stacking of the two phenyl groups in GHB-7 with nucleotides C25 and G5, indicating that hydrophobic interactions likely play a significant role in ligand binding. This is consistent with a preliminary quantitative structure–activity relationship study of 1,4-disubstituted 1,2,3-triazoles binding to AM1A.[9] It is also consistent with the binding studies (Section 2.1) which indicated that GHB-7 affinity was likely due to additional binding interactions beyond electrostatics. In addition, neither enantiomer had direct docking interactions with nucleotide C11, consistent with the similar affinity observed for GHB-7 binding AM1A and C11U (Section 2.1).

Interestingly, the *S*-GHB-7 phenyl groups stack on opposite sides of the G5:C25 base pair, essentially clamping the base pair between the two phenyl groups. This clamped stacking may result in additional stabilization of the secondary structure that would account for the increase in T_m observed for AM1A in the presence

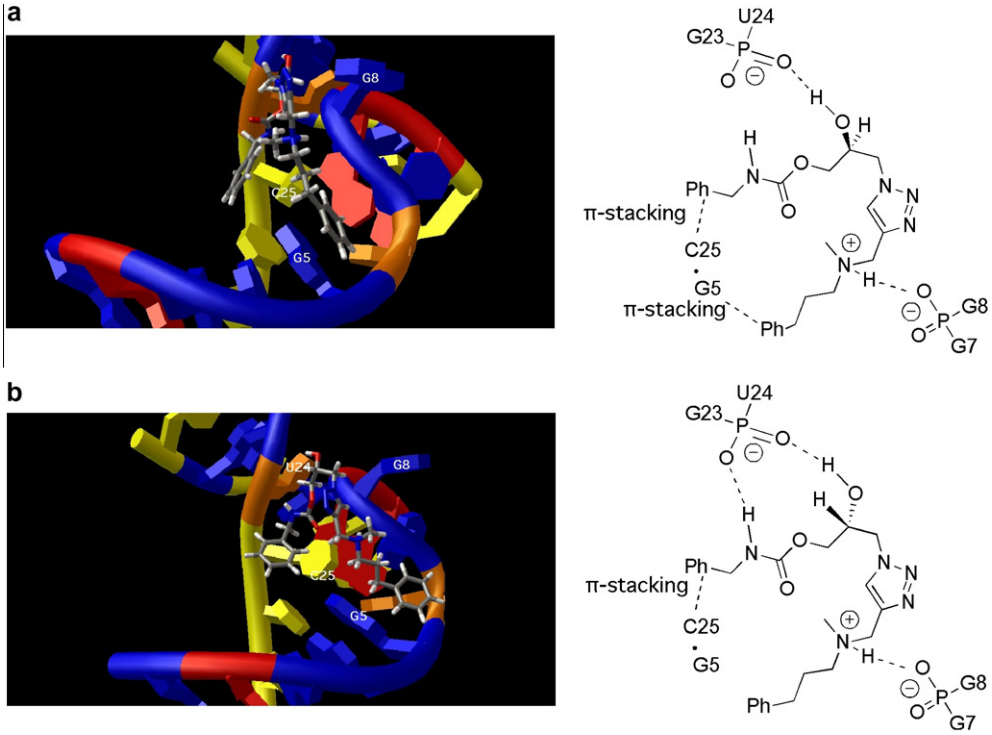

Figure. 4. Glide-derived docked structure and major contacts of GHB-7 binding to AM1A for (a) *S* and (b) *R* enantiomers. Nucleotide numbering according that shown in Figure 2a and dot represents G5:C25 base pair.

of GHB-7 (Section 2.2). The *R* enantiomer still has one of the phenyl groups stacking on C25, but rather than the other phenyl group stacking on G5, there is an additional hydrogen bond with a 5′-phosphate oxygen of U24. RNA binding studies with enantiomerically pure GHB-7 will need to be investigated in the future to determine if there is indeed a difference in binding modes for the two enantiomers. Recent studies with another set of ligands that bind AM1A have indicated that surface binding allows for enantiomers to make similar affinity contacts, but with differing functional group partners.[11] The docking of GHB-7 enantiomers appears to differ from this trend, most likely due to the ligand binding reaching into the helical region by stacking on opposite faces of the G5:C25 base pair, rather than simple surface binding along the grooves and phosphate backbone.

Limited aqueous solubility of GHB-7 precluded a detailed NMR study of the complex; however, imino proton spectral changes were investigated in a titration study with low concentrations of GHB-7. The solution structure of AM1A has been determined by NMR[24] and the structural effect of monovalent and divalent cations investigated.[25] Addition of GHB-7 to AM1A resulted in changes in the NMR spectra for the imino proton of G5 (Supplementary data). No other changes were observed. While solubility issues limited the final concentration of GHB-7 that could be investigated, the observed results are consistent with the docking studies that showed π–π stacking with G5.

3. Conclusion

The antiterminator element of the T box riboswitch is an intriguing drug discovery target given its high sequence conservation[15,16] and the critical role it plays in the regulation of key bacterial genes.[4] In this study, we investigated the molecular level interactions of a lead 1,4-disubstituted 1,2,3-triazole, GHB-7, binding to T box antiterminator model RNA, AM1A. GHB-7 binds in the bulge region of AM1A and stabilizes the secondary structure by making contacts that likely reach across the bulge nucleotides to the adjacent flanking helices, including a possible clamped π–π stacking interaction. This is in contrast to the AM1A surface binding observed for a series of 4,5-disubstituted oxazolidinones[11] indicating that this relatively simple RNA structural element is not predisposed to a single ligand binding mode. The implications of this for RNA drug discovery in general are significant because a range of binding modes, with similar affinity, can greatly complicate interpretation of structure–activity relationships in lead compound development. Evidence of multiple potential AM1A ligand binding modes complicating interpretation of structure–activity relationships has recently been observed.[12] This possibility needs to be considered in any comprehensive drug discovery project targeting relatively simple RNA structural elements such as bulges.

The studies reported here also explain a possible mechanism for the previously observed disruption of tRNA–antiterminator RNA complex formation by GHB-7.[12] Structural studies of T box antiterminator RNA have indicated that tRNA binds the antiterminator bulge nucleotides likely via induced fit and/or tertiary structure capture[24,26] and likely with no additional antiterminator contacts other than the known base pairing.[27,28] Since GHB-7 binds to the bulge region of the antiterminator and reduces the flexibility of the bulge nucleotides, it is reasonable that this would disrupt the contact points and flexibility requirements necessary for tRNA binding. These features will be important to investigate in the future for T box antiterminator-targeted RNA drug discovery.

4. Experimental section

4.1. Synthesis and preparation of GHB-7 and RNA

GHB-7 was synthesized as previously described.[9] Unlabeled antiterminator model RNAs AM1A and C11U were synthesized and dialyzed as previously described.[8,17] Fluorescently labeled AM1A and C11U used for K_d determinations were prepared or

purchased from Dharmacon, Inc. and dialyzed against 10 mM NaH_2PO_4 pH 6.5 0.01 mM EDTA prior to use as previously described.[6]

4.2. K_d determination

The fluorescence resonance energy transfer (FRET) monitored ligand binding assays were performed in a FLEXstation multiwell plate reader (Molecular Devices) as previously described.[6,7] FRET-labeled antiterminator model RNAs 3′Fl-AM1A/C11U-Rhd were renatured prior to use. Each experiment contained 100 nM FRET-labeled antiterminator model RNA, 50 mM NaCl, 5 mM $MgCl_2$, 0.01 mM EDTA, 12.5% DMSO with [GHB-7] ranging from 0 to 300 μM in a total volume of 100 μL. Following 130 min incubation at 25 °C, the FRET was monitored (λ_{ex} = 467 nm, λ_{em} = 585 nm) and the $F_{rel} = |F-F_0|/F_0$ was determined where F is the fluorescence at 585 nm in the presence of ligand and F_0 is in the absence of ligand. The binding isotherm for the average of duplicate data was fit to a single-site binding model using *Prism 5.0* (GraphPad).

4.3. UV-monitored thermal denaturation

UV-monitored thermal denaturation experiments were conducted as previously described[17,21] using a Beckman Coulter 640 UV/Vis spectrometer equipped with a peltier, temperature-controlled cell holder. RNA was renatured prior to use. The absorbance at 260 nm was monitored as the temperature was increased at a rate of 0.5 °C/min. Each experiment consisted of AM1A (0.7 μM) in 10 mM NaH_2PO_4, pH 6.5, 0.01 mM EDTA, 5% (v/v) DMSO either without or with GHB-7 (100 μM). To control for possible ligand absorbance, an identical experiment was run with ligand only (no RNA) and the resulting baseline was subtracted from the AM1A with GHB-7 data. The first derivative of the baseline corrected absorbance data was calculated using OD Deriv[29] and the T_m determined from peak dA/dT values.

4.4. In-line probing

In-line probing experiments were conducted as previously described.[11] AM1A was ^{32}P-5′-end-labeled using Kinase Max (Ambion). For the in-line probing experiments, 1 μL of labeled AM1A (~3000 CPM) was mixed with 5 μL of 2× in-line probing buffer (100 mM Tris–HCl, 200 mM KCl, 40 mM $MgCl_2$, pH 8.3) and 1 μL of GHB-7 stock solution (50:50 DMSO/H_2O) followed by dilution to a total volume of 10 μL with ddH_2O. The in-line probing experiments were incubated at room temperature (25 °C) for 40 h. The hydrolysis ladder reaction was assembled by adding 1 μL of labeled AM1A into 9 μL of hydrolysis buffer (50 mM Na_2CO_3 pH 9.2, 1 mM EDTA). This reaction was incubated at 90 °C for 15 min. To generate the RNase T1 ladder, 1 μL of labeled AM1A, 1 μL of carrier yeast RNA (3 μg/μL) and 7 μL of 1× sequencing buffer (20 mM sodium citrate pH 5.1, 1 mM EDTA and 7 M urea) were mixed and incubated at 50 °C for 5 min. Then 1 μL of 0.1 U/μL RNase T1 was added into the solution and incubated at room temperature for another 15 min. The resulting cleavage products were separated via 20% denaturing polyacrylamide gel electrophoresis (19:1 acrylamide/bis-acrylamide) and the bands visualized via autoradiography. The relative normalized band intensities were determined using Nucleo Vision (NucleoTech) and plotted against ligand concentration to determine the slope for ligand-induced relative band intensity changes as previously described.[11]

4.5. Ligand docking studies

Protonated GHB-7 was initially constructed in Spartan 04 (Wavefunction), energy minimized using molecular mechanics with MMFF[30] and the resulting structure exported to Macromodel (Schrödinger) for docking to the NMR-derived solution structure of AM1A (PDB ID = 1N53).[24] Ligand docking studies were conducted as previously described[11] using the Glide module of FirstDiscovery 2.7 (Schrödinger). Images of the resulting docked structures were rendered using PMV.[31]

Acknowledgments

We thank the NIH (GM073188) and Ohio University, through the BioMolecular Innovation & Technology (BMIT) project, for support of this work.

Supplementary data

Supplementary data associated with this article can be found, in the online version, at doi:10.1016/j.bmc.2011.12.017.

References and notes

1. Zhang, J.; Lau, M. W.; Ferre-D'Amare, A. R. *Biochemistry* **2010**, *49*, 9123.
2. Tucker, B. J.; Breaker, R. R. *Curr. Op. Struct. Biol.* **2005**, *15*, 342.
3. Smith, A. M.; Fuchs, R. T.; Grundy, F. J.; Henkin, T. M. *RNA Biol.* **2010**, *7*, 104.
4. Green, N. J.; Grundy, F. J.; Henkin, T. M. *FEBS Lett.* **2010**, *584*, 318.
5. Means, J. A.; Hines, J. V. *Bioorg. Med. Chem. Lett.* **2005**, *15*, 2169.
6. Means, J. A.; Katz, S. J.; Nayek, A.; Anupam, R.; Hines, J. V.; Bergmeier, S. C. *Bioorg. Med. Chem. Lett.* **2006**, *16*, 3600.
7. Anupam, R.; Bergmeier, S. C.; Green, N. J.; Grundy, F. J.; Henkin, T. M.; Means, J. A.; Nayek, A.; Hines, J. V. *Bioorg. Med. Chem. Lett.* **2008**, *18*, 3541.
8. Anupam, R.; Denapoli, L.; Muchenditsi, A. M.; Hines, J. V. *Bioorg. Med. Chem.* **2008**, *16*, 4466.
9. Acquaah-Harrison, G.; Zhou, S.; Hines, J. V.; Bergmeier, S. C. *J. Comb. Chem.* **2010**, *12*, 491.
10. Maciagiewicz, I.; Zhou, S.; Bergmeier, S. C.; Hines, J. V. *Bioorg. Med. Chem. Lett.* **2011**, 4524.
11. Orac, C. M.; Zhou, S.; Means, J. A.; Boehme, D.; Bergmeier, S. C.; Hines, J. V. *J. Med. Chem.* **2011**, 6786.
12. Zhou, S.; Acquaah-Harrison, G.; Bergmeier, S. C.; Hines, J. V. *Bioorg. Med. Chem. Lett.* **2011**, *21*, 7059.
13. Grundy, F. J.; Winkler, W. C.; Henkin, T. M. *Proc. Natl. Acad. Sci. USA* **2002**, *99*, 11121.
14. Grundy, F. J.; Yousef, M. R.; Henkin, T. M. *J. Mol. Biol.* **2005**, *346*, 73.
15. Gutierrez-Preciado, A.; Henkin, T. M.; Grundy, F. J.; Yanofsky, C.; Merino, E. *Microbiol. Mol. Biol. Rev.* **2009**, *73*, 36.
16. Vitreschak, A. G.; Mironov, A. A.; Lyubetsky, V. A.; Gelfand, M. S. *RNA* **2008**, *14*, 717.
17. Gerdeman, M. S.; Henkin, T. M.; Hines, J. V. *Nucleic Acids Res.* **2002**, *30*, 1065.
18. Mikkelsen, N. E.; Johansson, K.; Virtanen, A.; Kirsebom, L. A. *Nat. Struct. Biol.* **2001**, *8*, 510.
19. Tor, Y. *Chembiochem: Eur. J. Chem. Biol.* **2003**, *4*, 998.
20. Hermann, T.; Westhof, E. *J. Mol. Biol.* **1998**, *276*, 903.
21. Puglisi, J. D.; Tinoco, I., Jr. *Methods Enzymol.* **1989**, *180*, 304.
22. Zhou, S.; Acquaah-Harrison, G.; Jack, K. D.; Bergmeier, S. C.; Hines, J. V. *Chem. Biol. Drug Design* 2011, In press, doi:10.1111/j.1747-0285.2011.01274.x.
23. Regulski, E. E.; Breaker, R. R. *Methods Mol. Biol.* **2008**, *419*, 53.
24. Gerdeman, M. S.; Henkin, T. M.; Hines, J. V. *J. Mol. Biol.* **2003**, *326*, 189.
25. Jack, K. D.; Means, J. A.; Hines, J. V. *Biochem. Biophys. Res. Commun.* **2008**, *370*, 306.
26. Means, J. A.; Simson, C. M.; Zhou, S.; Rachford, A. A.; Rack, J.; Hines, J. V. *Biochem. Biophys. Res. Commun.* **2009**, *389*, 616.
27. Fauzi, H.; Agyeman, A.; Hines, J. V. *BBA-Gene Reg. Mech.* **2009**, *1789*, 185.
28. Fauzi, H.; Jack, K. D.; Hines, J. V. *Nucleic Acids Res.* **2005**, *8*, 2595.
29. Draper, D. E.; Gluick, T. C. *Methods Enzymol.* **1995**, *259*, 281.
30. Hehre, W. J.; Klunzinger, P. E. In *A Guide to Molecular Mechanics and Molecular Orbital Calculations in Spartan*; Wavefunction Inc.: Irvine, CA, 1997.
31. Sanner, M. F. *J. Mol. Graphics Mod.* **1999**, *17*, 57.